

Electrochemical performances of coal-based carbon prepared by low-temperature catalytic graphitization as anode materials for potassium-ion batteries

A. M. A. Mohamed^{a,b,*}, D. Cao^a, K. Zhu^a, K. Chand^a, M. Elhefnawy^{c,d}

^aKey Laboratory of Superlight Materials and Surface Technology, College of Material Science and Chemical Engineering, Harbin Engineering University, Harbin 150001, China

^bDepartment of Physics, Faculty of Education, University of Dongola, Sudan

^cInstitute of Materials Processing and Intelligent Manufacturing, College of Material Science and Chemical Engineering, Harbin Engineering University, Harbin 150001, China

^dDepartment of Mechanical Engineering, Kafrelsheikh University, Egypt

Potassium-ion batteries (PIBs) are promising as an attractive replacement to lithium-ion batteries (LIBs) on a wide storage energy stationary scale because of the abundance of potassium resources and easily accessible. Herein, we successfully prepared carbon anode materials for PIBs from a cheap and abundant coal by the low-temperature graphitization with $\text{Ni}(\text{CH}_3\text{COO})_2 \cdot 4\text{H}_2\text{O}$ catalyst. After 100 cycles, the coal-based carbon anode delivers a specific capacity of 200 mAh g^{-1} at 0.2 A g^{-1} current density, with more than 97% coulombic efficiency. This excellent potassium storage efficiency and the low cost make coal-based carbon anodes a most promising anode candidate for PIBs.

(Received August 8, 2021; Accepted November 4, 2021)

Keywords: Potassium-ion batteries, Catalytic graphitization, Coal-based carbon, Anodes materials

1. Introduction

Due to the growing attention to environmental and energy issues, the renewable energy requirements for energy storage equipment are increasing [1]; in recent years, lithium-ion batteries (LIBs) have become increasingly favored in the industry of energy storage [2] because of their advantages; for example, energy density, long life, and high working voltage [3]. (LIBs) were successfully used in electric automobiles [4] and mobile electronic devices [5]. Nevertheless, a high dependency on the (LIBs) is causing concern by the scarcity, and the increasing costs of lithium resources [6], due to the most easily reachable lithium reserves are in either distant or politically sensitive areas [7]. Therefore, secondary metal-ion batteries depend on the cheap and abundant earth elements (such as Na, Mg, Al, and K) that are widely taken into consideration [8]. In seeking the alternatives to LIBs, potassium-ion batteries (PIBs) and sodium-ion batteries (SIBs) have been proposed as two competitive candidates due to their similarities to LIBs [9]; potassium and sodium resources are much more abundant than lithium on the surface of the earth [10]. The K/K^+ couple have a redox potential closer to (-2.93 V vs standard hydrogen electrode) to that of Li/Li^+ (-3.04 V) than that of Na/Na^+ (-2.71 V) [11-13], indicating that PIBs have a higher energy density and higher discharge voltage plateau than SIBs [14]; from this viewpoint, PIBs would be a more acceptable choice as a low-cost alternative to LIBs. Graphite is a carbon allotrope composed of crystalline carbon; it was formed by stacking graphene layers. These graphene layers are comprised of a two-dimensional regular hexagon network, with an interlayer distance of 0.3354 nm between these sheets [15][16]. In contrast, the low-graphitization amorphous carbons mainly consist of amorphous surfaces and chaotic single layers of graphene [17]. Coal, a traditional fossil fuel [18], is well known as the most abundant and economical natural carbon source around the world, because of the character of its high carbon content (50% to 98%) [19]. Moreover, it is one of the world's most important energy sources representing 25% of its energy consumption [20]; as

* Corresponding authors: abdalland91@hotmail.com

we know, coal consists of graphitic crystalline domains connected with amorphous carbons that can further transform at high temperatures into artificial graphite [21], with pyrolyzed samples at $\sim 1000^\circ\text{C}$ under Ar gas; natural coal was reported as the anode of LIBs [22].

Therefore, for that, the preparation of coal for high-performance energy storage materials attracted considerable attention. Catalytic graphitization is a method in which a catalyst is used to improve the crystallization of carbon by a chemical reaction between the catalyst and ungraphitized carbon [23]; this method has been used with one of the transition metal elements, for instance, nickel (Ni), iron (Fe), copper (Cu), and cobalt (Co) [24], or metallic compounds, such as chromium oxide (Cr_2O_3) or manganese dioxide (MnO_2) [25], as a catalyst. Ni is especially effective from the catalysts mentioned above and has usually been used to obtain a graphitic structure with relatively high crystallinity [26]; using this method at low temperatures (under 1000°C), amorphous carbon materials can be graphitized.

In short, the commercial pure coal low-cost and the most abundant was converted by the catalytic graphitization with low-temperature from the amorphous structure into the crystalline structure as demonstrated in the results of transmission electron microscopy (TEM), X-ray diffraction (XRD), and Raman spectroscopy, to improve potassium ions storage. The coal-based carbon sample was tested as PIBs anode materials; the C800 anode achieved good electrochemical performance with a capacity of 200 mAh g^{-1} after 100 cycles at 0.2 A g^{-1} with coulombic efficiency of more than 97 % and good rate capability. This study has the following benefits: (i) the coal is a low-cost, readily available substance, (ii) the preparation method is flexible and scalable, and (iii) the obtained carbon show good performance in PIBs. As a result, coal-based carbon can be one of the most attractive carbon source candidates as anode materials for PIBs.

2. Experimental Work

2.1. Materials synthesis

Cleaned coal powder (400 mesh) and nickel (II) acetate tetrahydrate are used. Nickel (II) acetate was impregnated into ethanol (100 mL of 6 mmol metal salt concentration solution), mixed with 1 g of cleaned coal powder, and stirred at (600 rpm for 1 h), then a mixture solution was dried at 80°C for 24 h and then cool down to room temperature; after that, the mixed sample has been put into in crucible of corundum and put in the horizontal tube furnace then heated to 800°C with a heating rate of ($10^\circ\text{C min}^{-1}$) for 4 h under argon flow. Finally, coal-based carbons have been prepared and collected after natural cooling; it was denoted as C800 (represent coal and graphitization temperature) and PC (represent pure coal); after that, both samples were characterized by various techniques.

2.2. Materials Characterization

The coal powder underwent structural changes before and after catalytic graphitization as observed using X-ray diffraction (XRD) with $\text{CuK}\alpha$ radiation source ($\lambda = 1.5418\text{ \AA}$), and Raman spectroscopy (Horiba Jobin Yvon, LabRAM HR800, 532 nm, 17 mW, He-Ne laser excitation on 1800-line grating), and transmission electron microscopy (TEM, JEM-2100, JEOL model).

2.3. Electrochemical measurements

The slurry of the electrode was prepared by mixing active materials (PC or C800) with polyvinylidene fluoride (PVDF) as a binder and a carbon additive (Super P) with a ratio of weight (80:10:10) by using N-methyl pyrrolidone (NMP) solution as a solvent under magnetic stirring to form a homogeneous slurry. The mixture slurry was plated on the copper foil and then dried at 60°C under vacuum overnight. A dried copper foil has been cut into circle shapes with 12 mm in diameter, and by the weight difference, the mass of the active material was calculated. In an Ar-filled glove box, the coin cells CR2023-type were fabricated with the prepared electrode (used as an electrode) and potassium foil as a counter electrode. The electrolyte used was the 0.8 M KPF_6 in the mixture of ethylene carbonate (EC) and diethyl carbonate (DEC) in the volume ratio of (1:1) and with the separator of (Whatman) GF/C glassy fiber. All the cells were aged 24 hours before

measuring to ensure that the electrolyte was properly permeated into the electrodes. The galvanostatic charge and discharge analyses were performed by using a NEWARE battery test system (CT-4008 model) in the voltage window between 3.00 and 0.01 V, the Cyclic voltammetry (CV) and Electrochemical impedance spectroscopy (EIS) experiments were performed using (IVIUMnSTAT multichannel electrochemical analyser), (CV) scan rate at 0.1 mV s^{-1} , and (EIS) at a frequency ranging from 100 kHz to 10 mHz.

3. Results and discussion

To investigate the changes in the microstructures of the obtained samples XRD and Raman spectroscopy were applied. In Fig. 1(a), XRD patterns demonstrate two obvious diffraction peaks of coal-based carbon sample (C800) sharp (002) peak and a prominent (100) peak, In comparison to pure coal sample (PC), which indicates structural changes in the PC from an amorphous structure into a crystalline structure after applying catalytic graphitization. The first diffraction peak of the C800 sample located at 23.7° corresponds to the reflection in the (002), which indicating a random combination of graphitic stacking [27], the interlayer distance (d_{002}) of the C800 sample is 3.75 \AA which calculated by Bragg's law ($2d\sin\theta = n\lambda$), which is more than the interlayer distance of graphite (3.35 \AA) [28]. Thus, helping the insertion/extraction of K ions into the layered structure. The second diffraction peak of C800 can be seen at 2θ of 43.9° , corresponding to the (100) diffraction of disordered carbons structure [29]. Moreover, Raman spectroscopy has been used further to investigate the structures of C800 and PC samples. As shown in Fig. 1(b), Raman spectra contain two characteristic and independent peaks for the C800 sample at 1345 cm^{-1} (D-band) and 1590 cm^{-1} (G-band); the D band is related to the vibration of disordered carbon at the edges of the graphite sheets, while the G band corresponds to the in-plane C-C stretching vibration of graphitic carbon [30], while the two peaks are not clearly shown for the PC sample, which confirms the structural change after the catalytic graphitization and agreement with that of the XRD results. The degree of graphic disordering in carbon has been well established as the ID/IG ratio [31], the intensity ratio (ID/IG) of the C800 about 0.97, which indicates the increased graphitic degree with a catalytic graphitization at low temperature; also, these structures can be conducive to K ion storage in the coal-based carbon.

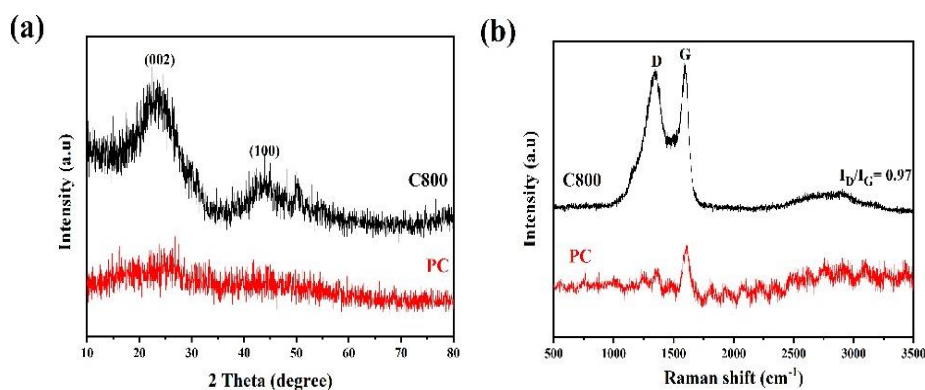


Fig. 1. (a) X-ray diffractions patterns of C800 and PC samples. (b) Raman spectrum of C800 and PC samples.

Transmission electron microscope (TEM) images confirmed the transformation of pure coal from an amorphous structure to a crystalline structure by catalytic graphitization. The TEM image in Fig. 2(a) reveals the amorphous structures of pure coal (PC). In contrast, the High-resolution TEM (HRTEM) micrographs for (C800) sample in Fig. 2(b) clearly shows that the coal-based carbon sample contains a crystalline structure with high ordered mixed with a small amount of amorphous carbon. This is due to increased temperature to $800 \text{ }^\circ\text{C}$; the active nickel particles

grow into amorphous coal particles and modify the structure of these particles to crystalline structure. This crystalline structure is also confirmed by the fast Fourier transform (FFT) image (upper Inset) in Fig. 2(b) that exhibits diffraction rings. Furthermore, the interlayer spacing (d_{002}), as shown in Fig. 2(b), is estimated at 0.375 nm; this layer spacing can provide sufficient sites for potassium ion insertion and extraction, giving a better electrochemical performance; these results consistent with the XRD and Raman analysis. Fig. 2(c) displays the TEM energy dispersive spectrometer (EDS) mapping images of the C800 sample, which illustrate the uniform and even distribution of nickel and carbon throughout the structure.

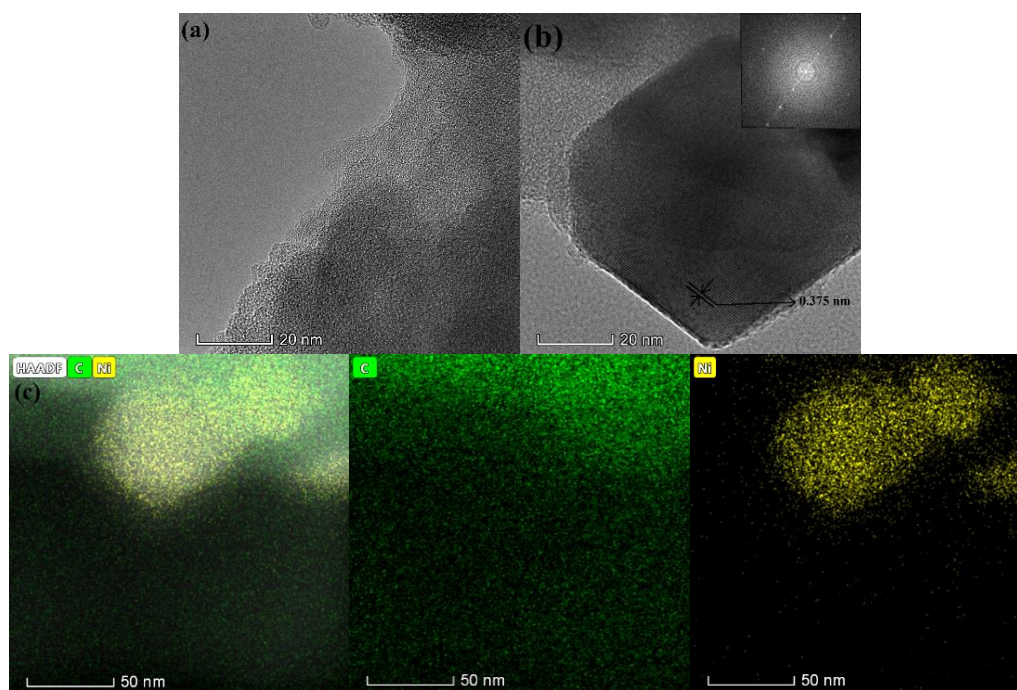


Fig. 2. Structural changes of coal after low temperature graphitization (a) TEM image of PC (b) HRTEM image and FFT image (inset) of C800 (c) EDS mapping images of the C800.

The pure coal sample (PC) and the coal-based carbon (C800) have been tested as electrodes in Potassium-ion batteries for assessing the potassium storage properties after catalytic graphitization. Galvanostatic charge-discharge measurements evaluated the electrochemical performance of both electrodes with a current density of 0.2 A g^{-1} at the voltage window between 0.01 and 3.0 V versus K^+/K . Fig.3 displays the discharge/charge profiles of the (RC) and (C800) electrodes for the initial three cycles, the first discharge and charge capacities of the coin cells with PC particles as a working electrode are 23.5 and 6 mAh g^{-1} , respectively Fig. 3(a) with initial coulombic efficiency (ICE) equivalent of 35.5%. In contrast, the coin cells with C800 particles as working electrode delivered capacities of 304 and 168 mAh g^{-1} (ICE:55%) in the initial discharge and charge cycle Fig. 3(b), which indicate better reversibility after catalytic graphitization, which contributed to the creation of additional sites of interaction for the graphitized samples, as expected from the XRD, Raman spectra, and TEM results.

To investigate the electrochemical performance of coal-based carbon, a variety of electrochemical measurements have been performed. Cyclic voltammetry (CV) has been used to investigate the K^+ intercalation /deintercalation in the C800 electrode, with a voltage window between 0.01 and 3.00 V vs K/K^+ and tested at 0.1 mV s^{-1} , as displayed in Fig. 4(a) one reduction peak able to be observed on the first cycle at 0.2 V indicating for electrolyte decomposition and the forming of the solid electrolyte interphase (SEI) films on the surface of the C800 sample, which is similar to the LIBs and SIBs method [32]. In the following cycles, this peak disappears, meaning that the stable SEI film was formed through the initial cycle. Moreover, the relatively sharp peak of oxidation at 0.25 V relates to the K^+ extraction from the defects and micropores of

the C800. The CV curves overlap well in the subsequent cycles, which indicate good stability of cycling and a large potassium capacitive storage ability.

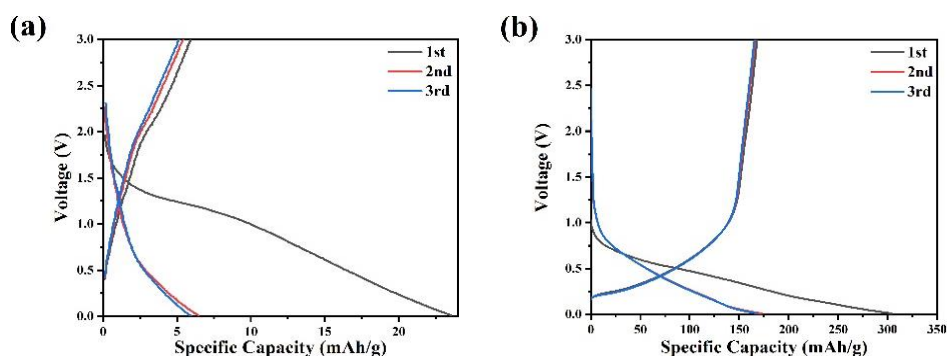


Fig. 3. Electrochemically comparative studies of PC and C800 as anodes of PIBs: Galvanostatic discharge and charge profiles of the initial three cycles of (a) PC and (b) C800 at 0.2 A g^{-1} current density.

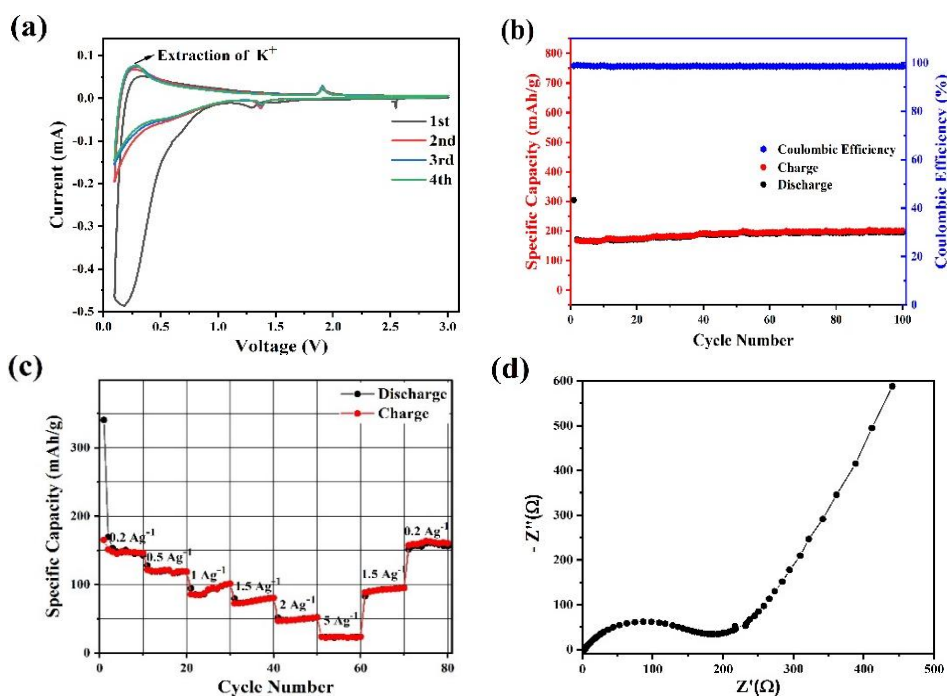


Fig. 4. Electrochemical evaluation of C800 anodes: (a) Cyclic voltammetry (CV) curves for the initial four cycles; (b) Cycling performance and coulombic efficiency in the voltage window between 0.01 and 3.0 V at the current rate of 0.2 A g^{-1} ; (c) Rate capacities at different current densities; (d) Nyquist plots after 50 cycles over the frequency range 10 mHz to 100 kHz.

The cycle performance and coulombic efficiency of C800 at 0.2 A g^{-1} as shown in Fig. 4(b), the C800 electrode was exhibiting good electrochemical reversibility through the (charge and discharge) cycles, after 100 cycles maintain the highest capacity of 200 mAh g^{-1} , with the coulombic efficiency of 98 % during cycling. The excellent cycle stability of the C800 material can be due to the wide surface and rich pores, which can provide more space for the potassium ion buffer.

The rate capacities performances of the C800 anode are displayed in Fig. 4(c) at different discharge/charge current densities, with 10 cycles at each rate, the reversible capacities of C800 at

0.2, 0.5, 1, 1.5, 2, and 5 A g⁻¹ are (average value in 10 cycles) 149, 119.7, 92.2, 76, 49, and 23.6 mAh g⁻¹, respectively. The capacity has been recovered to 160 mAh g⁻¹ after experiencing various charging/discharge rates, when the current density reverts to 0.2 A g⁻¹ after 70 cycles, demonstrating good reversibility. This excellent performance shows that the formed SEI and the electrodes during cycling are very stable.

Furthermore, the electrochemical impedance spectroscopy (EIS) measurement of the C800 anode was tested after 50 cycles, with a range frequency from 10 mHz to 100 kHz. As illustrated in Fig. 4(d), the Nyquist plots of C800 anode consisting of the semicircle at the high and middle-frequency range (represent the total resistances of contact and charge transfer) and a straight line at a low frequency range (describe the diffusion of potassium ion in the C800 electrode) [33].

4. Conclusions

In summary, the C800 anode was synthesized by the catalytic graphitization with a low-temperature method from coal and evaluated as anode materials for PIBs. The C800 anode exhibited cycling stability of 200 mAh g⁻¹ after 100 cycles at the current density of 0.2 A g⁻¹ with coulombic efficiency of more than 97 % and good rate performance. The good electrochemical performance and the potassium ions storage are attributed to the additional active sites formed after a structural change from amorphous to the crystalline structure, as evidenced by XRD, Raman spectra, and TEM characterizations results. In short, coal-based carbon anode materials will be promising anode material for PIBs in the future.

Acknowledgments

All authors thank the Harbin Engineering University China and the assistance of the Fundamental Research Funds for the Central Universities of China [HEUCF201732].

References

- [1] S. Yan, Q. Wang, S. Luo, Y. Zhang, X. Liu, J. Power Sources **461**, 228151 (2020).
- [2] Z. Wu, L. Wang, J. Huang, J. Zou, S. Chen, Electrochim. Acta **306**, 446 (2019).
- [3] M. Wang, Y. Zhu, Y. Zhang, J. Duan, K. Wang, J. Power Sources **481**, 228902 (2021).
- [4] K. Wu, Y. Feng, J. Huang, C. Bai, M. He, Chem. Phys. Lett. **756**, 137832 (2020).
- [5] Y. Du, T. Gao, W. Ma, H. Li, Chem. Phys. Lett. **712**, 7 (2018).
- [6] Z. Jian, W. Luo, and X. Ji, J. Am. Chem. Soc. **137**, 11566 (2015).
- [7] C. Zhang, Y. Xu, M. Zhou, L. Liang, H. Dong, M. Wu, Adv. Funct. Mater. **27**, 1604307 (2017).
- [8] B. Cao, Q. Zhang, H. Liu, B. Xu, S. Zhang, Adv. Energy Mater. **8**, 1801149 (2018).
- [9] S. Gong, Q. Wang, J. Phys. Chem. C **121**, 24418 (2017).
- [10] H. Wang, Q. Chen, H. Li, Q. Duan, D. Jiang, J. Hou, Chem. Phys. Lett. **735**, 136777 (2019).
- [11] M. Chen, W. Wang, X. Liang, S. Gong, J. Liu, Adv. Energy Mater. **8**, 1800171 (2018).
- [12] W. Wang, J. Zhou, Z. Wang, L. Zhao, P. Li, Adv. Energy Mater. **8**, 1701648 (2017).
- [13] Y. An, H. Fei, G. Zeng, L. Ci, B. Xi, J. Power Sources **378**, 66 (2018).
- [14] J. Ge, L. Fan, J. Wang, Q. Zhang, Z. Liu, Adv. Energy Mater. **8**, 1801477 (2018).
- [15] F. Destyorini, Y. Irmawati, A. Hardiansyah, H. Widodo, I. Yahya, Eng. Sci. Technol. an Int. J. **24**, 514 (2020).
- [16] M. Kakunuri, S. Kali, C. S. Sharma, Journal of Analytical and Applied **117**, 317 (2016).
- [17] X. Yu, K. Zhang, N. Tian, A. Qin, L. Liao, Mater. Lett. **142**, 193 (2015).
- [18] B. Xing, C. Zhang, Y. Cao, G. Huang, Q. Liu, Fuel Process. Technol. **172**, 162 (2018).
- [19] H. Shen, H. Zhao, M. Kang, W. Song, J. Ye, ChemElectroChem. **6**, 4541 (2019).

- [20] Y. Li, Y. Hu, X. Qi, X. Rong, H. Li, *Energy Storage Mater.* **5**, 191 (2016).
- [21] L. Sun, Z. Zhao, Y. Sun, X. Wang, X. Liu, *Diam. Relat. Mater.* **106**, 107827 (2020).
- [22] Abou-Rjeily, N. Laziz, C. Autret-Lambert, M. Sougrati, J. Toufaily, *Energy Technol.* **7**, 1900005 (2019).
- [23] C. J. Thambiliyagodage, S. Ulrich, P. T. Araujo, M. G. Bakker, *Carbon N. Y.* **134**, 452 (2018).
- [24] M. T. Johnson, K. T. Faber, *J. Mater. Res.* **26**, 18 (2011).
- [25] M. Sevilla, A. B. Fuertes, *Chem. Phys. Lett.* **490**, 63 (2010).
- [26] C. Chen, K. Sun, A. Wang, S. Wang, J. Jiang, *BioResources* **13**, 3165 (2018).
- [27] C. Gao, Q. Wang, S. Luo, Z. Wang, Y. Zhang, *J. Power Sources* **415**, 165 (2019).
- [28] Z. Ju, S. Zhang, Z. Xing, Q. Zhuang, Y. Qiang, *ACS Appl. Mater. Interfaces* **8**, 20682 (2016).
- [29] H. Hou, L. Shao, Y. Zhang, G. Zou, J. Chen, *Adv. Sci.* **4**, 1600243 (2016).
- [30] P. Li, J. Y. Hwang, S. M. Park, Y. K. Sun, *J. Mater. Chem. A* **6**, 12551 (2018).
- [31] J. Yang, Z. Ju, Y. Jiang, Z. Xing, B. Xi, J. Feng, *Adv. Mater.* **30**, 1700104 (2017).
- [32] H. Ma, X. Qi, D. Peng, Y. Chen, D. Wei, Z. Ju, *Chemistry Select* **4**, 11488 (2019).
- [33] J. Zhao, X. Zou, Y. Zhu, Y. Xu, C. Wang, *Adv. Funct. Mater.* **26**, 8103 (2016).